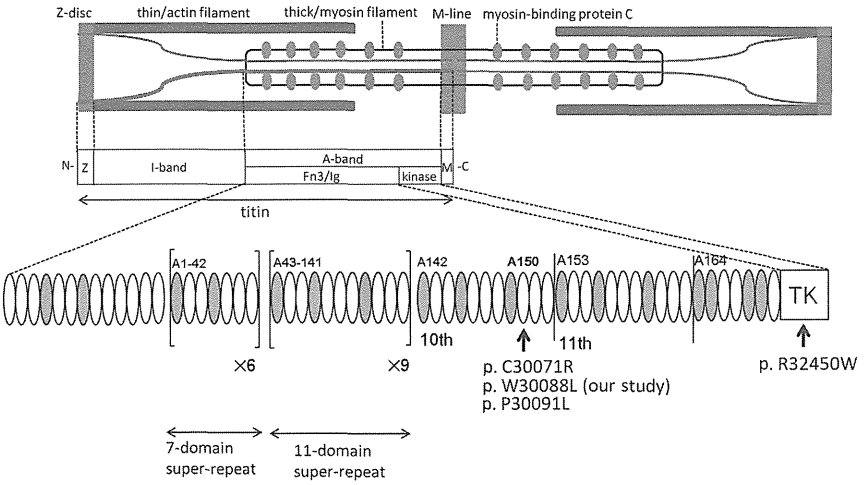

Figure 5 Structure of titin and mutation distribution in the A-band domain. Human *TTN* was mapped to 2q31.2. *TTN* is 294 kb and is composed of 363 exons that code for a maximum of 38 138 amino-acid residues and a 4.20-MDa protein[32] called titin. Titin is expressed in the cardiac and skeletal muscles and spans half the sarcomere, with its N-terminal at the Z-disc and the C-terminal at the M-line.[33] Titin is composed of four major domains: Z-disc, I-band, A-band and M-line. I-band regions of titin are thought to make elastic connections between the thick filament (that is, myosin filament) and the Z-disc within the sarcomere, whereas the A-band domain of titin seems to be bound to the thick filament, where it may regulate filament length and assembly.[34] The gray and white ellipses indicate an Ig-like domain and fibronectin type 3 domain, respectively. Our mutation (p.W30088L) and the neighboring two mutations (that is, p.C30071R and p.P30091L) were all located in the 6th Fn3 domain in the 10th domain of large super-repeats. A full color version of this figure is available at the *Journal of Human Genetics* journal online.

In contrast, one of the distinctive features of TMD is that early respiratory failure has not been observed in patients with TMD. Histological findings of TMD usually do not include CBs but show nonspecific dystrophic change. The underlying pathogenic processes explaining why mutations on these neighboring domains share some similarities but also some differences are unknown.

Three of four HMERF mutations in the A-band domain are located in the fibronectin type 3 and Ig-like (Fn3/Ig) domain, and one of four HMERF mutations is located in the kinase domain (Table 2, also see Figure 5). The missense mutation c.97348C>T in the kinase domain was the first reported HMERF mutation. It has been shown that the kinase domain has an important role in controlling muscle gene expression and protein turnover via the neighbor of BRCA1 gene-1-muscle-specific RING finger protein-serum response transcription factor pathway.[13] Moreover, the Fn3/Ig domain is composed of two types of super-repeats: six consecutive copies of 7-domain super-repeat at the N-terminus and 11 consecutive copies of 11-domain super-repeat at the C-terminus.[27–29] These super-repeats are highly conserved among species and muscles. Our identified mutation (c.90263G>T) and the neighboring two mutations (that is, c.90272C>T and c.90315T>C shown in Table 2) were all located on the 6th Fn3 domain in the 10th copy of 11-domain super-repeat (that is, A150 domain[30]) (Figure 5). Although some Fn3 domains are proposed to be the putative binding site for myosin,[31] the role with the majority of Fn3 domains, how it supports the structure of each repeat architecture, and the identity of its binding partner have not been fully elucidated. Our findings suggested that the Fn3 domain, in which mutations clustered, has critical roles in the pathogenesis of HMERF, although detailed mechanisms of pathogenesis remain unknown.

In conclusion, we have identified a novel disease-causing mutation in *TTN* in a family with MFM that was clinically compatible with HMERF. Because of its large size, global mutation screening of *TTN* has been difficult. Mutations in *TTN* may be detected by massively parallel sequencing in more patients with MFMs, especially in patients with early respiratory failure. Further studies are needed to understand the genotype–phenotype correlations in patients with mutations in *TTN* and the molecular function of titin.

ACKNOWLEDGEMENTS

We thank the patients and their family. We are grateful to Yoko Tateda, Kumi Kato, Naoko Shimakura, Risa Ando, Riyo Takahashi, Miyuki Tsuda, Nozomi Koshita, Mami Kikuchi and Kiyotaka Kuroda for their technical assistance. We also acknowledge the support of the Biomedical Research Core of Tohoku University Graduate School of Medicine. This work was supported by a grant of Research on Applying Health Technology provided by the Ministry of Health, Labor and Welfare to YM, an Intramural Research Grant (23-5) for Neurological and Psychiatric Disorders of NCNP and JSPS KAKENHI Grant number 24659421.

1 Nakano, S., Engel, A. G., Waclawik, A. J., Emslie-Smith, A. M. & Busis, N. A. Myofibrillar myopathy with abnormal foci of desmin positivity. I. Light and electron microscopy analysis of 10 cases. *J. Neuropathol. Exp. Neurol.* **55,** 549–562 (1996).
2 Olive, M., Odgerel, Z., Martinez, A., Poza, J. J., Bragado, F. G., Zabalza, R. J. *et al.* Clinical and myopathological evaluation of early- and late-onset subtypes of myofibrillar myopathy. *Neuromuscul. Disord.* **21,** 533–542 (2011).
3 Olive, M., Goldfarb, L. G., Shatunov, A., Fischer, D. & Ferrer, I. Myotilinopathy: refining the clinical and myopathological phenotype. *Brain* **128,** 2315–2326 (2005).
4 Selcen, D. & Engel, A. G. Myofibrillar myopathy caused by novel dominant negative alpha B-crystallin mutations. *Ann. Neurol.* **54,** 804–810 (2003).
5 Abe, K., Kobayashi, K., Chida, K., Kimura, N. & Kogure, K. Dominantly inherited cytoplasmic body myopathy in a Japanese kindred. *Tohoku. J. Exp. Med.* **170,** 261–272 (1993).
6 Abecasis, G. R., Cherny, S. S., Cookson, W. O. & Cardon, L. R. Merlin–rapid analysis of dense genetic maps using sparse gene flow trees. *Nat. Genet.* **30,** 97–101 (2002).
7 Li, H. & Durbin, R. Fast and accurate short read alignment with Burrows-Wheeler transform. *Bioinformatics* **25,** 1754–1760 (2009).
8 McKenna, A., Hanna, M., Banks, E., Sivachenko, A., Cibulskis, K., Kernytsky, A. *et al.* The Genome Analysis Toolkit: a MapReduce framework for analyzing next-generation DNA sequencing data. *Genome. Res.* **20,** 1297–1303 (2010).
9 Wang, K., Li, M. & Hakonarson, H. ANNOVAR: functional annotation of genetic variants from high-throughput sequencing data.. *Nucleic Acids Res.* **38,** e164 (2010).
10 Adzhubei, I. A., Schmidt, S., Peshkin, L., Ramensky, V. E., Gerasimova, A., Bork, P. *et al.* A method and server for predicting damaging missense mutations. *Nat. Methods* **7,** 248–249 (2010).
11 Nicolao, P., Xiang, F., Gunnarsson, L. G., Giometto, B., Edstrom, L., Anvret, M. *et al.* Autosomal dominant myopathy with proximal weakness and early respiratory muscle involvement maps to chromosome 2q. *Am. J. Hum. Genet.* **64,** 788–792 (1999).

12 Edstrom, L., Thornell, L. E., Albo, J., Landin, S. & Samuelsson, M. Myopathy with respiratory failure and typical myofibrillar lesions. *J. Neurol. Sci.* **96,** 211–228 (1990).
13 Lange, S., Xiang, F., Yakovenko, A., Vihola, A., Hackman, P., Rostkova, E. *et al.* The kinase domain of titin controls muscle gene expression and protein turnover. *Science* **308,** 1599–1603 (2005).
14 Ohlsson, M., Hedberg, C., Bradvik, B., Lindberg, C., Tajsharghi, H., Danielsson, O. *et al.* Hereditary myopathy with early respiratory failure associated with a mutation in A-band titin. *Brain* **135,** 1682–1694 (2012).
15 Pfeffer, G., Elliott, H. R., Griffin, H., Barresi, R., Miller, J., Marsh, J. *et al.* Titin mutation segregates with hereditary myopathy with early respiratory failure. *Brain* **135,** 1695–1713 (2012).
16 Vasli, N., Bohm, J., Le Gras, S., Muller, J., Pizot, C., Jost, B. *et al.* Next generation sequencing for molecular diagnosis of neuromuscular diseases. *Acta. Neuropathol.* **124,** 273–283 (2012).
17 Kontrogianni-Konstantopoulos, A., Ackermann, M. A., Bowman, A. L., Yap, S. V. & Bloch, R. J. Muscle giants: molecular scaffolds in sarcomerogenesis. *Physiol. Rev.* **89,** 1217–1267 (2009).
18 Ottenheijm, C. A. & Granzier, H. Role of titin in skeletal muscle function and disease. *Adv. Exp. Med. Biol.* **682,** 105–122 (2010).
19 Hackman, P., Vihola, A., Haravuori, H., Marchand, S., Sarparanta, J., De Seze, J. *et al.* Tibial muscular dystrophy is a titinopathy caused by mutations in TTN, the gene encoding the giant skeletal-muscle protein titin. *Am. J. Hum. Genet.* **71,** 492–500 (2002).
20 Udd, B., Partanen, J., Halonen, P., Falck, B., Hakamies, L., Heikkila, H. *et al.* Tibial muscular dystrophy. Late adult-onset distal myopathy in 66 Finnish patients. *Arch. Neurol.* **50,** 604–608 (1993).
21 de Seze, J., Udd, B., Haravuori, H., Sablonniere, B., Maurage, C. A., Hurtevent, J. F. *et al.* The first European family with tibial muscular dystrophy outside the Finnish population. *Neurology* **51,** 1746–1748 (1998).
22 Van den Bergh, P. Y., Bouquiaux, O., Verellen, C., Marchand, S., Richard, I., Hackman, P. *et al.* Tibial muscular dystrophy in a Belgian family. *Ann. Neurol.* **54,** 248–251 (2003).
23 Hackman, P., Marchand, S., Sarparanta, J., Vihola, A., Penisson-Besnier, I., Eymard, B. *et al.* Truncating mutations in C-terminal titin may cause more severe tibial muscular dystrophy (TMD). *Neuromuscul. Disord.* **18,** 922–928 (2008).
24 Pollazzon, M., Suominen, T., Penttila, S., Malandrini, A., Carluccio, M. A., Mondelli, M. *et al.* The first Italian family with tibial muscular dystrophy caused by a novel titin mutation. *J. Neurol.* **257,** 575–579 (2010).
25 Udd, B., Rapola, J., Nokelainen, P., Arikawa, E. & Somer, H. Nonvacuolar myopathy in a large family with both late adult onset distal myopathy and severe proximal muscular dystrophy. *J. Neurol. Sci.* **113,** 214–221 (1992).
26 Carmignac, V., Salih, M. A., Quijano-Roy, S., Marchand, S., Al Rayess, M. M., Mukhtar, M. M. *et al.* C-terminal titin deletions cause a novel early-onset myopathy with fatal cardiomyopathy. *Ann. Neurol.* **61,** 340–351 (2007).
27 Labeit, S., Barlow, D. P., Gautel, M., Gibson, T., Holt, J., Hsieh, C. L. *et al.* A regular pattern of two types of 100-residue motif in the sequence of titin. *Nature* **345,** 273–276 (1990).
28 Labeit, S. & Kolmerer, B. Titins: giant proteins in charge of muscle ultrastructure and elasticity. *Science* **270,** 293–296 (1995).
29 Tskhovrebova, L., Walker, M. L., Grossmann, J. G., Khan, G. N., Baron, A. & Trinick, J. Shape and flexibility in the titin 11-domain super-repeat. *J. Mol. Biol.* **397,** 1092–1105 (2010).
30 Bucher, R. M., Svergun, D. I., Muhle-Goll, C. & Mayans, O. The structure of the FnIII Tandem A77-A78 points to a periodically conserved architecture in the myosin-binding region of titin. *J. Mol. Biol.* **401,** 843–853 (2010).
31 Muhle-Goll, C., Habeck, M., Cazorla, O., Nilges, M., Labeit, S. & Granzier, H. Structural and functional studies of titin's fn3 modules reveal conserved surface patterns and binding to myosin S1–a possible role in the Frank-Starling mechanism of the heart. *J. Mol. Biol.* **313,** 431–447 (2001).
32 Bang, M. L., Centner, T., Fornoff, F., Geach, A. J., Gotthardt, M., McNabb, M. *et al.* The complete gene sequence of titin, expression of an unusual approximately 700-kDa titin isoform, and its interaction with obscurin identify a novel Z-line to I-band linking system. *Circ. Res.* **89,** 1065–1072 (2001).
33 Maruyama, K., Yoshioka, T., Higuchi, H., Ohashi, K., Kimura, S. & Natori, R. Connectin filaments link thick filaments and Z lines in frog skeletal muscle as revealed by immunoelectron microscopy. *J. Cell. Biol.* **101,** 2167–2172 (1985).
34 Guo, W., Bharmal, S. J., Esbona, K. & Greaser, M. L. Titin diversity–alternative splicing gone wild. *J. Biomed. Biotechnol.* **2010,** 753675 (2010).

Supplementary Information accompanies the paper on Journal of Human Genetics website (http://www.nature.com/jhg)

CLINICAL REPORT

AMERICAN JOURNAL OF medical genetics PART A

A Transient Myelodysplastic/Myeloproliferative Neoplasm in a Patient With Cardio-Facio-Cutaneous Syndrome and a Germline *BRAF* Mutation

Kazuhito Sekiguchi,[1]* Tomoki Maeda,[1] So-ichi Suenobu,[1,2] Nobutaka Kunisaki,[1] Miki Shimizu,[1] Kyoko Kiyota,[1] Yo-suke Handa,[1] Kensuke Akiyoshi,[1] Seigo Korematsu,[1,3] Yoko Aoki,[4] Yoichi Matsubara,[4] and Tatsuro Izumi[1]

[1]Department of Pediatrics and Child Neurology, Oita University Faculty of Medicine, Oita, Japan

[2]Division of General Pediatrics and Emergency Medicine, Oita University Faculty of Medicine, Oita, Japan

[3]Educational Support for Regional Pediatrics, Oita University Faculty of Medicine, Oita, Japan

[4]Department of Medical Genetics, Tohoku University School of Medicine, Sendai, Japan

Manuscript Received: 4 March 2013; Manuscript Accepted: 26 May 2013

A male infant, born at 32 weeks gestation by cesarean because of hydrops fetalis, presented with multiple anomalies, such as sparse and curly scalp hair, absent eyebrows, frontal bossing, an atrial septal defect, pulmonary artery stenosis, and whole myocardial thickening. He was clinically diagnosed with cardio-facio-cutaneous (CFC) syndrome, and was confirmed to have a germline V-raf murine sarcoma viral oncogene homologue B1 (*BRAF*) c.721 A>C mutation. At 1 month of age, he presented with a transient myelodysplastic/myeloproliferative neoplasm (MDS/MPN), which improved within a month without the administration of antineoplastic agents. This is the first report of CFC syndrome with MDS/MPN. The coexistence of MDS/MPN may be related to this *BRAF* c.721 A>C mutation. © 2013 Wiley Periodicals, Inc.

Key words: cardio-facio-cutaneous syndrome; myelodysplastic/myeloproliferative neoplasm; BRAF; RAS/MAPK syndromes; juvenile myelomonocytic leukemia

How to Cite this Article:
Sekiguchi K, Maeda T, Suenobu S-I, Kunisaki N, Shimizu M, Kiyota K, Handa Y-S, Akiyoshi K, Korematsu S, Aoki Y, Matsubara Y, Izumi T. 2013. A transient myelodysplastic/myeloproliferative neoplasm in a patient with cardio-facio-cutaneous syndrome and a germline BRAF mutation.
Am J Med Genet Part A 161A:2600–2603.

INTRODUCTION

Cardio-facio-cutaneous (CFC) syndrome is genetic disorder characterized by clinical features such as congenital heart defects, a characteristic facial appearance, ectodermal abnormalities and growth failure [Reynolds et al., 1986]. V-raf murine sarcoma viral oncogene homolog B1 (*BRAF*) is one of rat sarcoma viral oncogene homolog/mitogen activated protein kinase (RAS/MAPK) signaling pathway genes, and has been identified as a causative gene of CFC syndrome [reviewed in Aoki et al., 2008 and Denayer and Legius, 2007]. We report on a male infant with CFC syndrome, who was confirmed to have a germline *BRAF* mutation, and then presented with a myelodysplastic/myeloproliferative neoplasm (MDS/MPN) at 1 month of age.

CLINICAL REPORT

A male was born through cesarean at 32 weeks gestation as the first product of healthy nonconsanguineous Japanese parents. His birth weight, length and head circumference were 2,370 g (−0.8 SD), 40.0 cm (+2.3 SD), 34.2 cm (+3.2 SD), respectively. Due to hydrops fetalis and neonatal asphyxia, he required immediate resuscitation. Mechanical ventilation was needed until age 3 months. He presented with multiple anomalies, such as sparse and curly scalp hair, absent eyebrows, frontal bossing with temporal narrowing, ocular hypertelorism, low set ears, a short and webbed neck, and cryptorchidism (Fig. 1). His complete blood counts at age 1 day revealed the following: WBC 12,770/μl (neutrophils 80%,

Conflict of interest: none.

*Correspondence to:
Kazuhito Sekiguchi, Department of Pediatrics and Child Neurology, Oita University Faculty of Medicine, 1-1 Idaigaoka, Hasama, Yufu, Oita 879-5593, Japan.
E-mail: sekiguch@oita-u.ac.jp

Article first published online in Wiley Online Library (wileyonlinelibrary.com): 15 August 2013
DOI 10.1002/ajmg.a.36107

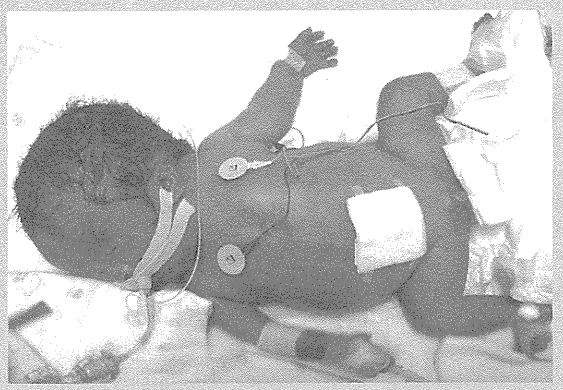

FIG. 1. Full-body image of the patient at birth and his facial features at 3 hours of age. The patient showed severe generalized edema at birth. He presented with sparse and curly hair, frontal bossing, hypertelorism, low-set ears, a short and webbed neck, and cryptorchidism.

lymphocytes 12%, monocytes 6%, myelocytes 2%), RBC 343 × 10^4/μl, erythroblasts 2,430/μl, hemoglobin 14.2g/dl, and platelets 3.2 × 10^4/μl. A chromosome analysis of his peripheral blood lymphocytes showed a 46, XY karyotype. He had an atrial septal defect (ASD), pulmonary artery stenosis (PS), whole myocardial thickening, a pulmonary arteriovenous fistula, an intrahepatic portal systemic shunt, hepatosplenomegaly, right cryptorchidism, a right double renal pelvis, and ureter and agenesis of the corpus callosum. These clinical features were all compatible with CFC syndrome.

At age 1 month, a peripheral blood examination indicated monocytosis of 17% (2,370/μl), with WBC 13,930/μl, RBC 295 × 10^4/μl, and platelets 11.2 × 10^4/μl, with giant platelets. Bone marrow aspiration revealed a nucleated cell count of 9.4 × 10^4/μl, megakaryocyte count 56.2/μl, and did not contain pathologic blasts. The karyotype of the bone marrow cells was 46, XY. The granulocyte-macrophage colony-forming unit (CFU-GM) assay using a semi-solid methylcellulose method showed spontaneous CFU-GM formation of bone marrow (5/5 × 10^4 mononuclear cells) and peripheral blood (35/5 × 10^4 mononuclear cell), without growth factors. Based on these laboratory findings, this patient was diagnosed with MDS/MPN. However, the peripheral blood monocytosis improved without the administration of antineoplastic agents after 1 month with 13% monocytes (1,140/μl), WBC of 8,780/μl, RBC 314 × 10^4/μl, and platelets 26.3 × 10^4/μl. At age 3 years, his complete blood counts revealed 11% monocytes (903/μl), WBC 8,210/μl, RBC 428 × 10^4/μl, and platelets 31.1 × 10^4/μl (Table I). He smiled normally. He demonstrated generalized hypotonia without normal head control and was unable to produce meaningful speech.

CYTOGENETIC AND GENOMIC ANALYSIS

The *BRAF* sequencing analysis showed a heterozygous A>C change at nucleotide 721, resulting in a p.T241P amino acid change in exon 6, which was a previously known mutation in CFC syndrome [Schulz et al., 2008]. No mutations were noted in the Kirsten rat sarcoma viral oncogene homologue (*KRAS*) or protein-tyrosine phosphatase, nonreceptor-type11 (*PTPN11*).

DISCUSSION

A male infant, born via cesarean section because of hydrops fetalis, presented with multiple anomalies suggestive of CFC syndrome. A pulmonary arteriovenous fistula, an intrahepatic portal systemic shunt, hepatosplenomegaly, cryptorchidism, a double renal pelvis, and ureter have been reported as rare complications in CFC syndrome [Narumi et al., 2007]. At 1 month of age, he presented with MDS/MPN, which improved within a month. He showed a germline mutation of *BRAF* c.721 A>C, resulting in a p.T241P amino acid change in exon 6, within a cysteine-rich domain. This mutation was previously described in CFC syndrome [Schulz et al., 2008].

The clinical findings of CFC syndrome are similar to those of other RAS/MAPK or neuro-cardio-facial-cutaneous syndromes, such as Noonan and Costello syndrome [reviewed in Aoki et al., 2008; Denayer and Legius, 2007]. The RAS/MAPK signaling pathway genes, not only *BRAF*, but also *KRAS*, MAPK kinase/ERK kinase 1 (*MEK1*), and MAPK kinase/ERK kinase2 (*MEK2*) have been reported as causative genes for CFC syndrome [Niihori et al., 2006; Rodriguez-Viciana et al., 2006]. CFC syndrome had been considered to have a low risk of malignancy among the various RAS/MAPK syndromes, but a few patients with CFC syndrome due to *BRAF* mutation have presented with malignancies, such as acute lymphoblastic leukemia [van Den Berg and Hennekam, 1999; Makita et al., 2007], and precursor T-lymphoblastic lymphoma [Ohtake et al., 2011].

MDS/MPNs include clonal myeloid neoplasms that at the time of initial presentation have clinical, laboratory or morphologic findings supporting a diagnosis of MDS, and other findings more consistent with MPN. They are usually characterized by hypercellularity of the

TABLE I. Peripheral Blood Examinations of This Patient

Age (months)	0	1	2	12	21	38
WBC (/μl)	12,770	13,930	8,730	8,660	9,040	8,210
Monocytes (/μl)	766	2,370	1,140	866	633	903
RBC (×10^4/μl)	343	295	314	396	404	428
Platelets (×10^4/μl)	3.2	11.2	26.3	24.2	38.6	31.1

bone marrow due to proliferation in one or more of the myeloid lineages [Swerdlow et al., 2008]. Juvenile myelomonocytic leukemia (JMML) is one type of MDS/MPN. Peripheral blood and bone marrow from JMML patients demonstrate spontaneous proliferation according to a CFU-GM assay [Estrov et al., 1986]. Transient monocytosis is not rare in preterm infants [Rajadurai et al., 1992]. Monocytosis in preterm infants is not usually considered a sign of MPD/MPN. In this case, the monocytes proliferation independent of growth factors was noticed according to a CFU-GM assay. The spontaneous proliferation was in favor of MPN. In RAS/MAPK syndromes, occasionally young infants with Noonan syndrome develop a JMML-like disorder which spontaneously resolves without treatment in some, and behaves more aggressively in others [Bader-Meunier et al., 1997; reviewed in Choong et al., 1999]. These children carried germline mutations in *PTPN11* [Tartaglia et al., 2003] or in *KRAS* [Kratz et al., 2005]. *BRAF* mutations had not previously been detected in patients with JMML [de Vries et al., 2007]. This is the first report of a germline *BRAF* mutation and MDS/MPN in a patient with CFC syndrome. The MDS/MPN improved without the administration of antineoplastic agents. This clinical course is similar to the JMML-like disorder observed in Noonan syndrome. This suggests a common mechanism for the development and progression of MDS/MPN in patients with RAS/MAPK syndromes. The MDS/MPN in RAS/MAPK syndrome patients has parallels with the transient leukemia of newborns with Down syndrome. However, the transient leukemia associated with Down syndrome has a high concentration of blasts in the peripheral blood and a GATA binding protein 1 (*GATA1*) mutation as somatic molecular marker [Xu et al., 2003].

The germline *BRAF* mutation site of this patient, c.721 A>C in exon 6, had been reported in two previous patients. One had CFC syndrome [Schulz et al., 2008], and the other had Noonan syndrome with multiple lentigines, previously referred to as LEOPARD syndrome [Sarkozy et al., 2009]. These two patients did not present with malignancies. Garnett and Marais [2004] reviewed the *BRAF* mutations in various adult cancers, and showed that up to 90% of mutations occurred in exon 12. The *BRAF* mutation site of this patient, exon 6, may be related to the spontaneous improvement of his MDS/MPN. A long-term follow-up and additional bone marrow assays might be needed if the patient demonstrates suspicious symptoms with or without peripheral blood monocytosis, because of the risk that MDS/MPN may recur. Further accumulated data about CFC syndrome with a *BRAF* mutation may help to elucidate the basic mechanisms of malignancy, and may suggest a therapeutic strategy.

ACKNOWLEDGMENTS

The authors are grateful to Drs. Hideki Muramatsu and Seiji Kojima, Department of Pediatrics/Developmental Pediatrics, Nagoya University Graduate School of Medicine, Nagoya, for providing important data from the colony assay.

REFERENCES

Aoki Y, Niihori T, Narumi Y, Kure S, Matsubara Y. 2008. The RAS/MAPK syndromes: novel roles of the RAS pathway in human genetic disorders. Hum Mutat 29:992–1006. Review.

Bader-Meunier B, Tchernia G, Miélot F, Fontaine JL, Thomas C, Lyonnet S, Lavergne JM, Dommergues JP. 1997. Occurrence of myelodysplastic/myeloproliferative neoplasm in patients with Noonan syndrome. J Pediatr 130:885–889.

Choong K, Freedman MH, Chitayat D, Kelly EN, Taylor G, Zipursky A. 1999. Juvenile myelomonocytic leukemia and Noonan syndrome. J Pediatr Hematol Oncol 21:523–527. Review.

de Vries AC, Stam RW, Kratz CP, Zenker M, Niemeyer CM, van den Heuvel-Eibrink MM. European Working Group on childhood MDS (EWOG-MDS). 2007. Mutation analysis of the *BRAF* oncogene in juvenile myelomonocytic leukemia. Haematologica 92:1574–1575.

Denayer E, Legius E. 2007. What's new in the neuro-cardio-facial-cutaneous syndromes? Eur J Pediatr 166:1091–1098. Review.

Estrov Z, Grunberger T, Chan HS, Freedman MH. 1986. Juvenile chronic myelogenous leukemia: characterization of the disease using cell cultures. Blood 67:1382–1387.

Garnett MJ, Marais R. 2004. Guilty as charged: *B-RAF* is a human oncogene. Cancer Cell 6:313–319. Review.

Kratz CP, Niemeyer CM, Castleberry RP, Cetin M, Bergsträsser E, Emanuel PD, Hasle H, Kardos G, Klein C, Kojima S, Stary J, Trebo M, Zecca M, Gelb BD, Tartaglia M, Loh ML. 2005. The mutational spectrum of *PTPN11* in juvenile myelomonocytic leukemia and Noonan syndrome/myeloproliferative disease. Blood 106:2183–2185.

Makita Y, Narumi Y, Yoshida M, Niihori T, Kure S, Fujieda K, Matsubara Y, Aoki Y. 2007. Leukemia in Cardio-facio-cutaneous (CFC) syndrome: a patient with a germline mutation in *BRAF* proto-oncogene. J Pediatr Hematol Oncol 29:287–290.

Narumi Y, Aoki Y, Niihori T, Neri G, Cavé H, Verloes A, Nava C, Kavamura MI, Okamoto N, Kurosawa K, Hennekam RC, Wilson LC, Gillessen-Kaesbach G, Wieczorek D, Lapunzina P, Ohashi H, Makita Y, Kondo I, Tsuchiya S, Ito E, Sameshima K, Kato K, Kure S, Matsubara Y. 2007. Molecular and clinical characterization of cardio-facio-cutaneous (CFC) syndrome: Overlapping clinical manifestations with Costello syndrome. Am J Med Genet Part A 143A:799–807.

Niihori T, Aoki Y, Narumi Y, Neri G, Cavé H, Verloes A, Okamoto N, Hennekam RC, Gillessen-Kaesbach G, Wieczorek D, Kavamura MI, Kurosawa K, Ohashi H, Wilson L, Heron D, Bonneau D, Corona G, Kaname T, Naritomi K, Baumann C, Matsumoto N, Kato K, Kure S, Matsubara Y. 2006. Germline *KRAS* and *BRAF* mutations in cardio-facio-cutaneous syndrome. Nat Genet 38:294–296.

Ohtake A, Aoki Y, Saito Y, Niihori T, Shibuya A, Kure S, Matsubara Y. 2011. Non-Hodgkin lymphoma in a patient with cardiofaciocutaneous syndrome. J Pediatr Hematol Oncol 33:e342–e346.

Rajadurai VS, Chambers HM, Vigneswaran R, Gardiner AA. 1992. Monocytosis in preterm infants. Early Hum Dev. 28:223–229.

Reynolds JF, Neri G, Herrmann JP, Blumberg B, Coldwell JG, Miles PV, Opitz JM. 1986. New multiple congenital anomalies/mental retardation syndrome with cardio-facio-cutaneous involvement—The CFC syndrome. Am J Med Genet 25:413–427.

Rodriguez-Viciana P, Tetsu O, Tidyman WE, Estep AL, Conger BA, Cruz MS, McCormick F, Rauen KA. 2006. Germline mutations in genes within the MAPK pathway cause cardio-facio-cutaneous syndrome. Science 311:1287–1290.

Sarkozy A, Carta C, Moretti S, Zampino G, Digilio MC, Pantaleoni F, Scioletti AP, Esposito G, Cordeddu V, Lepri F, Petrangeli V, Dentici ML, Mancini GM, Selicorni A, Rossi C, Mazzanti L, Marino B, Ferrero GB, Silengo MC, Memo L, Stanzial F, Faravelli F, Stuppia L, Puxeddu E, Gelb BD, Dallapiccola B, Tartaglia M. 2009. Germline *BRAF* mutations in Noonan, LEOPARD, and cardiofaciocutaneous syndromes: Molecular diversity and associated phenotypic spectrum. Hum Mutat 30:695–702.

Schulz AL, Albrecht B, Arici C, van der Burgt I, Buske A, Gillessen-Kaesbach G, Heller R, Horn D, Hübner CA, Korenke GC, König R, Kress W, Krüger G, Meinecke P, Mücke J, Plecko B, Rossier E, Schinzel A, Schulze A, Seemanova E, Seidel H, Spranger S, Tuysuz B, Uhrig S, Wieczorek D, Kutsche K, Zenker M. 2008. Mutation and phenotypic spectrum in patients with cardio-facio-cutaneous and Costello syndrome. Clin Genet 73:62–70.

Swerdlow SH, Campo E, Harris NL, Jaffe ES, Pileri SA, Stein H, Thiele J, Vardiman JW. 2008. World Health Organization classification of tumours of haematopoietic and lymphoid tissues. Lyon: International Agency for Research on Cancer.

Tartaglia M, Niemeyer CM, Fragale A, Song X, Buechner J, Jung A, Hählen K, Hasle H, Licht JD, Gelb BD. 2003. Somatic mutations in *PTPN11* in juvenile myelomonocytic leukemia, myelodysplastic syndromes and acute myeloid leukemia. Nat Genet 34:148–150.

van Den Berg H, Hennekam RC. 1999. Acute lymphoblastic leukaemia in a patient with cardiofaciocutaneous syndrome. J Med Genet 36:799–800.

Xu G, Nagano M, Kanezaki R, Toki T, Hayashi Y, Taketani T, Taki T, Mitui T, Koike K, Kato K, Imaizumi M, Sekine I, Ikeda Y, Hanada R, Sako M, Kudo K, Kojima S, Ohneda O, Yamamoto M, Ito E. 2003. Frequent mutations in the *GATA-1* gene in the transient myeloproliferative disorder of Down syndrome. Blood 102:2960–2968.

Hepatology Research

Hepatology Research 2013 doi: 10.1111/hepr.12168

Short Communication

Sequential analysis of amino acid substitutions with hepatitis B virus in association with nucleoside/nucleotide analog treatment detected by deep sequencing

Masashi Ninomiya,[1] Yasuteru Kondo,[1] Tetsuya Niihori,[2] Takeshi Nagashima,[3] Takayuki Kogure,[1] Eiji Kakazu,[1] Osamu Kimura,[1] Yoko Aoki,[2] Yoichi Matsubara[2] and Tooru Shimosegawa[1]

[1]Division of Gastroenterology, Tohoku University Hospital, [2]Department of Medical Genetics, and [3]Division of Cell Proliferation, Tohoku University Graduate School of Medicine, Sendai, Japan

Taking nucleoside/nucleotide analogs is a major antiviral therapy for chronic hepatitis B infection. The problem with this treatment is the selection for drug-resistant mutants. Currently, identification of genotypic drug resistance is conducted by molecular cloning sequenced by the Sanger method. However, this methodology is complicated and time-consuming. These limitations can be overcome by deep sequencing technology. Therefore, we performed sequential analysis of the frequency of drug resistance in one individual, who was treated with lamivudine on-and-off therapy for 2 years, by deep sequencing. The lamivudine-resistant mutations at rtL180M and rtM204V and the entecavir-resistant mutation at rtT184L were detected in the first subject. The lamivudine- and entecavir-resistant strain was still detected in the last subject. However, in the deep sequencing analysis, rt180 of the first subject showed a mixture in 76.9% of the methionine and in 23.1% of the leucine, and rt204 also showed a mixture in 69.0% of the valine and 29.8% of the isoleucine. During the treatment, the ratio of resistant mutations increased. At rt184, the resistant variants were detectable in 58.7% of the sequence, with the replacement of leucine by the wild-type threonine in the first subject. Gradually, entecavir-resistant variants increased in 82.3% of the leucine in the last subject. In conclusion, we demonstrated the amino acid substitutions of the serial nucleoside/nucleotide analog resistants. We revealed that drug-resistant mutants appear unchanged at first glance, but actually there are low-abundant mutations that may develop drug resistance against nucleoside/nucleotide analogs through the selection of dominant mutations.

Key words: amino acid substitutions, deep sequencing, hepatitis B virus, nucleoside/nucleotide analog resistants

Approximately 350–400 million patients are chronically infected with hepatitis B virus (HBV) globally, and the disease has caused epidemics in East Asia.[1,2] In Japan, approximately 1.5 million people are infected with HBV.[3] Chronic hepatitis B (CHB) increases the risk of liver cirrhosis and hepatocellular carcinoma.[4]

Hepatitis B virus is a DNA virus of 3.2 kb surrounded by an envelope of the surface protein (hepatitis B surface antigen [HBsAg]) and it has a circular genome of partially double-stranded DNA.[5] Once the HBV invades into hepatic cells, genomic DNA is transferred to the cell nucleus.[6] In the nucleus, the genomic DNA is converted to a stable intrahepatic reservoir of cccDNA. The cccDNA replicates through an RNA intermediate form by reverse transcription.[7] The purpose of CHB therapy is to achieve sustained suppression of HBV replication and the remission of liver disease. However, cccDNA is resistant to treatment and is not completely eradicated by currently available medications.[8,9] Taking nucleoside/nucleotide analogs (NA) is a major antiviral therapy for the treatment of CHB.[4] Therapies with NA available in Japan include lamivudine (LAM), adefovir dipivoxil (ADV) and entecavir (ETV). They inhibit viral polymerase activity by interfering with the priming of reverse transcription and elongation of the viral minus or plus strand DNA.[10–12] Most patients have chemical and virological responses, but these treatments are hampered by the selection of drug-resistant mutants, leading

Correspondence: Dr Yasuteru Kondo, Division of Gastroenterology, Tohoku University Hospital, 1-1 Seiryo, Aoba-ku, Sendai 980-8574, Japan. Email: yasuteru@ebony.plala.or.jp

The GenBank/EMBL/DDBJ accession numbers for the nucleotide sequences reported in this paper are AB820840-AB820852.

Received 7 March 2013; revision 14 May 2013; accepted 20 May 2013.

to a loss of efficacy, viral relapse and exacerbations of hepatitis after discontinuation.[13]

In the present study, the region of codon rt148 to rt 208 in the polymerase open reading frame was found to include the reported relevant NA-resistant amino acid substitutions. Resistance to LAM has been mapped to the YMDD locus in the C domain of rtM204I/V and is sometimes associated with compensatory mutations in the B domain of rtL180M and/or rtV173L.[14–16] The mutations common to LMV confer cross-resistance and reduced sensitivity to ETV but not to ADV. ETV resistance has been mapped to the B domain with rtI169T, rtL180M and/or rtT184S/A/I/L/F/G/C/M, C domain with rtS202C/G/I and rtM204V/I, and E domain of rtM250I/L/V. The three amino acid substitutions of rtL180 + rtM204 and either rtT184, rtS202 or rtM250 are required for ETV resistance to develop.[17–19] The mutations in the B domain of rtA181S/T/V and D domain of rtN236T were reported to be associated with ADV resistance.[20,21]

Currently, identification of HBV genotypic NA resistance is mainly conducted by polymerase chain reaction (PCR) amplification with Sanger direct sequencing. However, with this method it is difficult to measure the frequencies of each mutation, and it is impossible to detect several mutations combined in the same sequence. It is necessary to find the frequencies of NA-resistant amino acid substitutions, because the secondary compensatory mutations associated with primary NA resistance may restore replication defects or even give rise to multidrug-resistant variants.[19] As an alternative to Sanger direct sequencing, molecular cloning can analyze single viral DNA molecules. However, this methodology is complicated and time-consuming, because analysis of three-digit clones is required to detect variants present in several percent of quasispecies. These limitations can now be overcome by deep sequencing technology.[22] Genetic diversity plays a key role in the NA treatment of HBV infection. Therefore, using this technology, minor HBV variants can be detected, including those with combinations of nucleotide changes in the same period. Detecting low-frequency NA resistants will be important for choosing the NA treatment. In this study, we investigated the transition frequency of amino acid substitutions in NA resistants, in one case using deep sequencing during 2 years of ETV and ADV combination treatment.

A 42-year-old man, diagnosed with CHB infection in June 2005, was treated with LAM on-and-off therapy for 2 years. In HIV-infected patients, on-and-off antiretroviral therapy increased the risk of drug resistance compared with continuous therapy.[23] The HBV DNA levels had gradually increased and ETV treatment was begun in November 2007, but the HBV DNA levels did not decrease, and the treatment was stopped in November 2009. The level of serum transaminase was not elevated at that period. In April 2010, he was seen for the first time in our hospital. The patient was asymptomatic but showed an elevation of transaminase. The following clinical data was indicated: aspartate aminotransferase, 66 IU/L; alanine aminotransferase (ALT), 178 IU/L; positive for HBsAg, hepatitis B e-antigen (HBeAg) and hepatitis B core antibody; HBV genotype C; HBV DNA levels of 1.0×10^8 copies/mL; and negative for anti-hepatitis C virus and anti-HIV. The combination of ETV (0.5 mg/day) and ADV (10 mg/day) therapy was started at that time. After 3 months of therapy, the ALT elevation (119 IU/L) still persisted. Then, the dose of ETV was increased from 0.5 mg to 1.0 mg daily from August 2010. Three months after starting ETV at a dose of 1.0 mg, ALT was at 40 IU/L and HBV DNA had decreased to 6.3×10^3 copies/mL. At the most recent follow up, ALT has remained normal and HBV DNA is at nearly an undetectable level ($<1.3 \times 10^2$ copies/mL). Of note, the serum level of HBeAg is still positive. The changes in viral load and ALT levels are presented in Figure 1(a).

To investigate mutation involved in NA resistance, six serial serum samples of HBV-P10140 (stored in April 2010), HBV-P10193 (June 2010), HBV-P10234 (July 2010), HBV-P10264 (August 2010), HBV-P11021 (January 2011) and 12-009 (January 2012) were enrolled in this study. We extracted HBV DNA by the method described previously with slight modification.[24] Nucleic acids were obtained from 100 μL serum samples using SMITEST EX-R&D (Medical & Biological Laboratories, Nagoya, Japan) and nested PCR was conducted in the presence of PrimeSTAR HS DNA polymerase (TaKaRa Bio, Shiga, Japan) four with primers targeting the polymerase gene of HBV genomes (Table 1). The amplification product of the first-round PCR was 457 bp (nt 596–1052), and that of the second-round PCR was 390 bp (nt 610–999): the nucleotide numbers are in accordance with a genotype B HBV isolate of 3215 nt (accession no. AB010289). The first-round PCR with primers B034 and B037 was conducted for 30 cycles and the second-round PCR for 25 cycles with primers B035 and B036 (Table 1). The second-round PCR amplicons were sequenced directly on both strands using a BigDye Terminator version 3.1 Cycle Sequencing Kit (Applied Biosystems, Foster City, CA, USA) on a 3500xL Genetic Analyzer (Applied Biosystems).

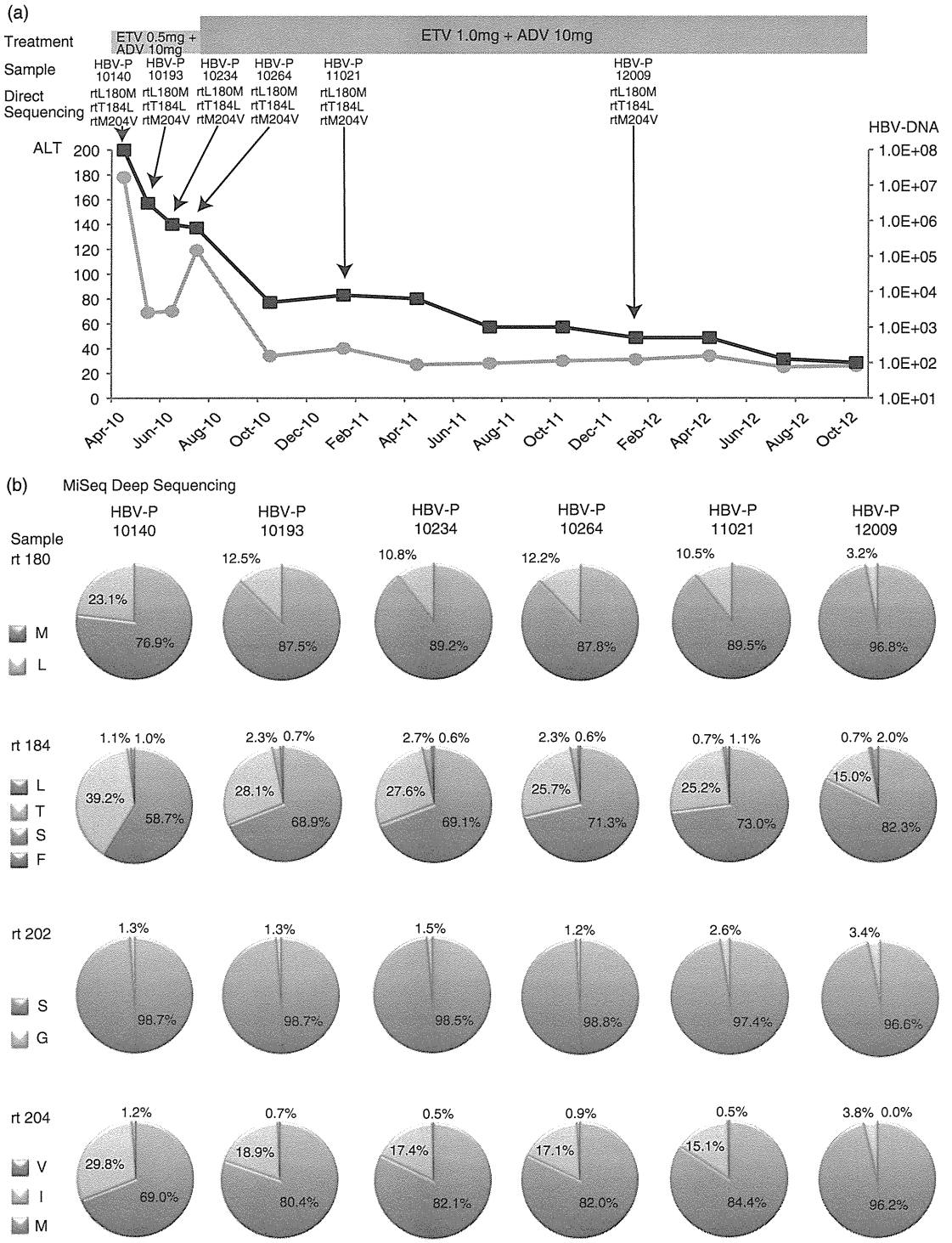

Figure 1 Clinical stage and amino acid substitutions of hepatitis B virus (HBV) resistants. (a) Evolution of HBV DNA viral load, alanine aminotransferase (ALT) levels and resistant HBV variants sequenced directly with Sanger methods in a patient treated sequentially with entecavir (ETV) and adefovir dipivoxil (ADV). (b) Frequency of amino acid substitutions of nucleoside/nucleotide analog (NA)-resistant HBV by MiSeq deep sequencing. M denotes methionine, L denotes leucine, T denotes threonine, V denotes valine, S denotes serine, F denotes phenylalanine, G denotes glycine and I denotes isoleucine. —■—, HBV-DNA; —●—, ALT.

Table 1 Nucleotide sequence of oligonucleotide primers

Primer	Polarity	Usage	Nucleotide sequence
B034	Sense	1st PCR	ACYTGTATTCCCATCCCATC
B037	Antisense	1st PCR	AARGCAGGRTADCCACATTG
B035	Sense	2nd PCR	CCCATCRTCYTGGGCTTTCG
B036	Antisense	2nd PCR	AATTCKYTGACATACTTTCCAATC
P5_B035	Sense	MiSeq sequence	AATGATACGGCGACCACCGAGATCTACACTC TTTCCCTACACGACGCTCTTCCGATCT*CCCA TCRTCYTGGGCTTTCG*
P7_Index1_B036	Antisense	MiSeq sequence of HBV-P10140	CAAGCAGAAGACGGCATACGAGAT***CGTGAT***G TGACTGGAGTTCAGACGTGTGCTCTTCCGA TCT*AATTCKYTGACATACTTTCCAATC*
P7_Index2_B036	Antisense	MiSeq sequence of HBV-P10193	CAAGCAGAAGACGGCATACGAGAT***ACATCG***G TGACTGGAGTTCAGACGTGTGCTCTTCCGAT *CTAATTCKYTGACATACTTTCCAATC*
P7_Index3_B036	Antisense	MiSeq sequence of HBV-P10234	CAAGCAGAAGACGGCATACGAGAT***GCCTAA***GT GACTGGAGTTCAGACGTGTGCTCTTCCGATCT *AATTCKYTGACATACTTTCCAATC*
P7_Index4_B036	Antisense	MiSeq sequence of HBV-P10264	CAAGCAGAAGACGGCATACGAGAT***TGGTCA***GTG ACTGGAGTTCAGACGTGTGCTCTTCCGATCTAA *TTCKYTGACATACTTTCCAATC*
P7_Index5_B036	Antisense	MiSeq sequence of HBV-P11021	CAAGCAGAAGACGGCATACGAGAT***CACTGT***GTG ACTGGAGTTCAGACGTGTGCTCTTCCGATCTAA *TTCKYTGACATACTTTCCAATC*
P7_Index6_B036	Antisense	MiSeq sequence of HBV-P12009	CAAGCAGAAGACGGCATACGAGAT***ATTGGC***GTGA CTGGAGTTCAGACGTGTGCTCTTCCGATCTAATT *CKYTGACATACTTTCCAATC*

Y denotes C or T, R denotes A or G, D denotes A, G or T and K denotes G or T. Italic bold letters indicate the index by multiplex sequencing. Italic letters indicate the nucleotide sequence of B035 or B036.
PCR, polymerase chain reaction.

The LAM-resistant mutations at rtL180M and rtM204V, and the ETV-resistant mutation at rtT184L in HBV-P10140 were detected by direct sequencing. The HBV-mutated LAM- and ETV-resistant strain was still detected in HBV-P12009 and the amino acid substitutions were the same in all subjects (Fig. 1a).

Next, we investigated the frequency of amino acid bases with these same six PCR amplicons by MiSeq (Illumina, San Diego, CA, USA) deep sequencing. MiSeq is the only deep sequencer that quickly integrates amplification, sequencing and data analysis in a single instrument. Compared with HiSeq (Illumina) or Illumina GA IIx, MiSeq can produce longer paired-end reads ($<2 \times 250$) with fewer gigabases of data. However, it has a large enough data volume to sequence PCR amplicons.

A second PCR was performed to attach the required sequencing adaptor for Illumina Miseq sequencing protocol as well as barcode to allow multiplexing of multiple sample libraries per sequencing lane. Six pairs of primers tailed with the adaptor and the specific index were used to amplify six first PCR amplicons. Eight cycles of PCR were performed using PrimeSTAR HS DNA polymerase. All adaptor–barcode–primers are shown in Table 1. The PCR amplicons were purified using AMPure XP beads (Beckman Coulter, Danvers, MA, USA) and the quality and quantity were checked by size range analysis using a D1K ScreenTape on the 2200 Tapestation (Agilent Technologies, Santa Clara, CA, USA). Each library was pooled in equal amounts, and a PhiX control kit (Illumina) was added to 95% of the pooled libraries. Sequencing was performed on MiSeq (Illumina) using 251-bp paired-end reads. Fastq files including demultiplexed sequence reads were generated by Miseq reporter. 251-bp paired-end reads were stripped of low quality 3′-regions using trim galore (www.bioinformatics.babraham.ac.uk/projects/trim_galore/). Sequence reads were aligned with the HBV reference sequence of Yamagata-1 (accession no. AB010289) using of Bowtie 2 (2.1.0).[25] The analysis

Table 2 Number of reads and read depth of each sample

Sample	HBV-P10140	HBV-P10193	HBV-P10234	HBV-P10264	HBV-P11021	HBV-P12009
No. of reads mapping on HBV reference	187 336	186 386	166 257	158 781	169 709	137 139
Read depth	88 985	87 825	76 775	75 296	80 190	65 095

of the read depth and base count is displayed using GATK (www.broadinstitute.org/gatk/).

A total of 1 005 608 validated reads corresponding to six serial samples were analyzed by deep sequencing. The mean number of reads mapping on the HBV reference was 167 601 and the mean depth of each case was 79 028 (Table 2). The nine most variable amino acid substitutions, rt169, rt173, rt180, rt181, rt184, rt202, rt204, rt236 and rt250, known to be associated with NA resistance, were examined. The problem was how to differentiate true mutations from sequencing error in the obtained reads. Nishijima *et al.* tried to determine the PCR amplicon of the HBV genome derived from the expression plasmid to take the PCR-induced errors as well as sequencing errors into consideration. They described that the mean error rate was 0.034%, with the distribution of the per-nucleotide error rate ranging 0–0.13%.[26] Therefore, mutations over 1.0% were considered to be valid. First, rt180 of HBV-P10140 showed mixed variants in 76.9% of methionine with LAM-resistant mutations and in 23.1% of wild type with leucine, and rt204 also showed mixed variants in 69.0% of valine and 29.8% of isoleucine with LAM-resistant mutations, and in only 1.2% of wild-type methionine. During the NA treatment, the ratio of resistance mutations was increased, and rt180 of HBV-P12009 showed mixed variants in 96.8% of methionine with LAM-resistant mutations and rt204 also showed mixed variants in 96.2% of valine with LAM-resistant mutations. At rt184, related to ETV resistance, the resistant variants were detectable in 58.7% of the sequence, with replacement of leucine by wild-type threonine in HBV-P10140. Gradually, ETV-resistant variants increased and were detected in 82.3% of leucine in HBV-P12009. In addition, at rt202, the ration of serine with ETV mutants was increased from 1.3% to 3.4% during the treatment with NA (Fig. 1b). Of note, at rt169, rt173, rt181, rt236 and rt250, there were no NA-resistant mutations.

Then, we investigated the existence of drug-resistant HBV clones that could latently develop in patients. We enrolled seven patients treated with continuous NA for up to 2 years but in whom there was continual detection of viral copies in serum in this trial. Direct Sanger sequencing detected LAM-resistant mutations in five of the seven subjects. They had the following mutations: (i) rtL180M + rtM204V and (ii) rt180M and no mutations were found at rtV173L. However, by deep sequencing, in four subjects there was part of a mixture with rtL180L/M (35.4%/64.6%) and rtM204M/V (35.2%/64.8%) in HBV-P10036, with rtL180L/M (10.6%/86.8%) and rtM204M/V/I (0.0%/75.5%/24.5%) in HBV-P12043, with rtL180L/M (19.5%/80.5%) and rtM204M/V/I (4.4%/79.5%/16.1%) in HBV-P13064 and with rtL180L/M (23.4%/76.6%), rtM204M/V/I (23.2%/41.6%/35.2%) and one secondary minority variant of rtV173V/L (55.4%/44.6%) in HBV-P13061. Next, an ADV-resistant mutation of rtA181V was detected in two subjects by Sanger sequencing, and was present in 100.0% in HBV-P07061 and in 35.3% in HBV-P08463 by deep sequencing. In addition, minority variant ADV-resistant mutations were detected with 8.5% of rtA181V and with 14.5% of rtN236T in HBV-P10036, and with 2.1% of rtA181V in HBV-P13064. Of note, an ETV-resistant mutation appeared only in one subject with rtT184L by Sanger sequencing, while some low frequency ETV-resistant mutations were detected in four subjects by deep sequencing (Table 3). Therefore, the continual viremia of HBV treated with NA for long term may lead to NA-resistant mutations.

In conclusion, we demonstrated the amino acid substitutions of serial NA-resistant HBV by Sanger sequencing and MiSeq deep sequencing. We revealed that NA-resistant mutants appear unchanged at a glance but suggest the existence of low-abundant mutant clones that may develop drug resistance against NA through the selection of dominant mutations. The viral loads have decreased, but the effect of ETV is expected to be reduced. Further analysis by deep sequencing technologies is necessary to understand the significance and clinical relevance of viral mutations in the pathophysiology of NA-resistant HBV infection.

Table 3 HBV NA-resistant mutations detected by Sanger sequencing and deep sequencing

Sample	Treatment	HBV DNA (log copies/mL)	NA-resistant mutations	
			Sanger sequence	Deep sequence
HBV-P07061	LAM + ADV	5.0	A181V	**A181V (100.0%)**
HBV-P10036	ETV	2.5	L180M, M204V	V173M (1.3%), **L180M (64.6%), A181V (8.5%), T184S (4.5%), S202C (2.3%), M204V (64.8%), N236T (14.3%)**
HBV-P08463	ETV	3.4	A181V	**A181V (35.3%)**
HBV-P12043	ETV	4.7	L180M, M204V	V173M (4.4%), **V173L (2.7%), L180M (86.8%)**, L180Q (2.6%), **T184L (27.9%), T184M (5.1%), S202G (16.6%), M204V (75.5%), M204I (24.5%)**
HBV-P12081	LAM + ADV	2.9	L180M, T184L, M204V	I169A (25.4%), **L180M (100.0%), T184L (100.0%), M204V (100.0%)**
HBV-P13064	ETV	7.1	L180M, M204V	V173M (12.9%), **L180M (80.5%), A181V (2.1%), A181T (3.6%), M204V (79.5%), M204I (16.1%), M250L (2.8%)**
HBV-P13061	ETV	2.3	L180M	**V173L (44.6%), L180M (76.6%), M204V (41.6%), M204I (35.2%), M250L (1.3%)**

Mutations in bold type at deep sequence section showed NA-resistant mutations that have already been reported.
ADV, adefovir dipivoxil; ETV, entecavir; HBV, hepatitis B virus; LAM, lamivudine; NA, nucleoside/nucleotide analog.

REFERENCES

1 EASL clinical practice guidelines: management of chronic hepatitis B virus infection. *J Hepatol* 2012; **57:** 167–85.
2 Pan CQ, Hu KQ, Tsai N. Long-term therapy with nucleoside/nucleotide analogues for chronic hepatitis B in Asian patients. *Antivir Ther* 2012; doi: 10.3851/IMP2481. [Epub ahead of print].
3 Yokosuka O, Kurosaki M, Imazeki F *et al.* Management of hepatitis B: consensus of the Japan Society of Hepatology 2009. *Hepatol Res* 2011; **41:** 1–21.
4 Lok ASF, McMahon BJ. Chronic hepatitis B: update 2009. *Hepatology* 2009; **50:** 661–2.
5 Zuckerman AJ. Hepatitis viruses. In: Baron S, ed. *Medical Microbiology*, 4th edn. Galveston (TX): University of Texas Medical Branch at Galveston, 1996; Chapter 70.
6 Kann M, Bischof A, Gerlich WH. In vitro model for the nuclear transport of the hepadnavirus genome. *J Virol* 1997; **71:** 1310–16.
7 Locarnini S. Molecular virology of hepatitis B virus. *Semin Liver Dis* 2004; **24** (Suppl 1): 3–10.
8 Werle-Lapostolle B, Bowden S, Locarnini S *et al.* Persistence of cccDNA during the natural history of chronic hepatitis B and decline during adefovir dipivoxil therapy. *Gastroenterology* 2004; **126:** 1750–8.
9 Wong DK, Yuen MF, Ngai VW, Fung J, Lai CL. One-year entecavir or lamivudine therapy results in reduction of hepatitis B virus intrahepatic covalently closed circular DNA levels. *Antivir Ther* 2006; **11:** 909–16.
10 Severini A, Liu XY, Wilson JS, Tyrrell DL. Mechanism of inhibition of duck hepatitis B virus polymerase by (-)-beta-L-2′,3′-dideoxy-3′-thiacytidine. *Antimicrob Agents Chemother* 1995; **39:** 1430–5.
11 Seigneres B, Aguesse-Germon S, Pichoud C *et al.* Duck hepatitis B virus polymerase gene mutants associated with resistance to lamivudine have a decreased replication capacity in vitro and in vivo. *J Hepatol* 2001; **34:** 114–22.
12 Seifer M, Hamatake RK, Colonno RJ, Standring DN. In vitro inhibition of hepadnavirus polymerases by the triphosphates of BMS-200475 and lobucavir. *Antimicrob Agents Chemother* 1998; **42:** 3200–8.
13 Inada M, Yokosuka O. Current antiviral therapies for chronic hepatitis B. *Hepatol Res* 2008; **38:** 535–42.
14 Allen MI, Deslauriers M, Andrews CW *et al.* Identification and characterization of mutations in hepatitis B virus resistant to lamivudine. Lamivudine Clinical Investigation Group. *Hepatology* 1998; **27:** 1670–7.
15 Fu L, Cheng YC. Role of additional mutations outside the YMDD motif of hepatitis B virus polymerase in L(-)SddC (3TC) resistance. *Biochem Pharmacol* 1998; **55:** 1567–72.
16 Fu L, Liu SH, Cheng YC. Sensitivity of L-(-)2,3-dideoxythiacytidine resistant hepatitis B virus to other antiviral nucleoside analogues. *Biochem Pharmacol* 1999; **57:** 1351–9.
17 Tenney DJ, Levine SM, Rose RE *et al.* Clinical emergence of entecavir-resistant hepatitis B virus requires additional substitutions in virus already resistant to Lamivudine. *Antimicrob Agents Chemother* 2004; **48:** 3498–507.
18 Tenney DJ, Rose RE, Baldick CJ *et al.* Long-term monitoring shows hepatitis B virus resistance to entecavir in

nucleoside-naive patients is rare through 5 years of therapy. *Hepatology* 2009; **49:** 1503–14.
19 Locarnini S. Primary resistance, multidrug resistance, and cross-resistance pathways in HBV as a consequence of treatment failure. *Hepatol Int* 2008; **2:** 147–51.
20 Bartholomeusz A, Tehan BG, Chalmers DK. Comparisons of the HBV and HIV polymerase, and antiviral resistance mutations. *Antivir Ther* 2004; **9:** 149–60.
21 Yatsuji H, Suzuki F, Sezaki H *et al.* Low risk of adefovir resistance in lamivudine-resistant chronic hepatitis B patients treated with adefovir plus lamivudine combination therapy: two-year follow-up. *J Hepatol* 2008; **48:** 923–31.
22 Ninomiya M, Ueno Y, Funayama R *et al.* Use of illumina deep sequencing technology to differentiate hepatitis C virus variants. *J Clin Microbiol* 2012; **50:** 857–66.
23 Danel C, Moh R, Chaix ML *et al.* Two-months-off, four-months-on antiretroviral regimen increases the risk of resistance, compared with continuous therapy: a randomized trial involving West African adults. *J Infect Dis* 2009; **199:** 66–76.
24 Takahashi M, Nishizawa T, Gotanda Y *et al.* High prevalence of antibodies to hepatitis A and E viruses and viremia of hepatitis B, C, and D viruses among apparently healthy populations in Mongolia. *Clin Diagn Lab Immunol* 2004; **11:** 392–8.
25 Langmead B, Salzberg SL. Fast gapped-read alignment with Bowtie 2. *Nat Methods* 2012; **9:** 357–9.
26 Nishijima N, Marusawa H, Ueda Y *et al.* Dynamics of hepatitis B virus quasispecies in association with nucleos(t)ide analogue treatment determined by ultra-deep sequencing. *PLoS ONE* 2012; **7:** e35052.

A Case of Almost Unilateral Focal Dermal Hypoplasia Resulting From a Novel Mutation in the *PORCN* Gene

Masayuki Asano[1], Taku Fujimura[1]*, Chihiro Wakusawa[1], Yoko Aoki[2], Yoichi Matsubara[2] and Setsuya Aiba[1]
*Departments of [1]Dermatology, and [2]Medical Genetics, Tohoku University Graduate School of Medicine, Seiryo-machi 1-1, Aoba-ku, Sendai, 980-8574, Japan. *E-mail: tfujimura1@mac.com*
Accepted April 11, 2012.

Focal dermal hypoplasia (FDH), also known as Goltz syndrome, is an X-linked dominant disorder of ecto-mesenchymal development. In general, FDH presents with characteristic linear streaks of hypoplastic dermis and various abnormalities in some organs (1). Although this disorder is normally lethal in male patients, approximately 10% of cases of FDH are male, and most represent post-zygotic mosaicism (2–4).

The molecular basis of FDH involves mutations in the *PORCN* (human porcupine locus MG61/PORC) gene (5). *PORCN* is a member of the porcupine (porc) gene family and is located on chromosome Xp11. 23 (1, 6). The gene is thought to encode an O-acyltransferase that catalyses cysteine N-palmitoylation and serine O-acylation in the endoplasmic reticulum that allows membrane targeting and secretion of several Wnt proteins that have key roles in embryonic tissue development, notably for fibroblast proliferation and osteogenesis (1, 7).

We describe here a case of FDH with a novel deletion mutation at exon 14 (c.1179_1193 del) detected by PCR-sequencing analysis of the entire coding sequences of the *PORCN* gene. Interestingly, in this case, the characteristic symptom was prominent in the patient's left hemibody. To the best of our knowledge, this is the second case report that reveals a mutation of the PORCN gene in a patient with almost unilateral FDH.

CASE REPORT

A 2-year-old Japanese girl visited our outpatient clinic for hypopigmented and atrophic linear skin lesions on the trunk and extremities. She had been surgically treated one year before for syndactyly of the left middle and ring finger. On her first visit to our hospital, physical examination disclosed hypo-pigmented patches of dermal hypoplasia distributed along Blaschko's lines on the arms, legs and trunk (Fig. 1). Interestingly, these symptoms in lesions were prominent on her left hemibody. Her hair was sparse and brittle and she had non-scarring alopecia. In addition, extensive dental caries was noted. From the above information, we diagnosed this patient as having almost unilateral FDH.

To confirm the diagnosis, we examined the *PORCN* gene for mutations. After receiving informed consent, DNA was extracted from the peripheral blood sample taken from affected individual using standard methods. Primers were designed to amplify individual exons and the flanking intron of the *PORCN* gene, as described previously (1). PCR-sequencing analysis of the entire coding sequences of *PORCN* revealed c.1179_1193 del mutation at exon 14 (Fig. 2). This variant was predicted to result in altered residues 394–412 and to produce a truncated protein (p.G394 fs X20). The sequence chromatograms showed low signal intensities at the site of mutation, indicating post-zygotic mutation. To verify the mosaic state, the PCR products were cloned into the pCR4 TOPO TA Cloning Vector (Invitrogen, Karlsruhe, Germany), transfected. *E. coli* clones were chosen and subjected to colony PCR, and PCR products from individual clones were sequenced. By DNA sequence analysis of selected clones we could assign the wild-type and the mutant sequence to either of the 2 banding patterns and identified a ratio of 5/26 (~19%; mutant vs. wild-type sequence).

DISCUSSION

FDH is characterized by linear and whorled lesions of hypoplastic dermis and variable abnormalities of organs including the bone, nails, hair, limbs and teeth (1–3). Cutaneous features that predominate at birth are red atrophic, linear lesions following Blaschko's lines

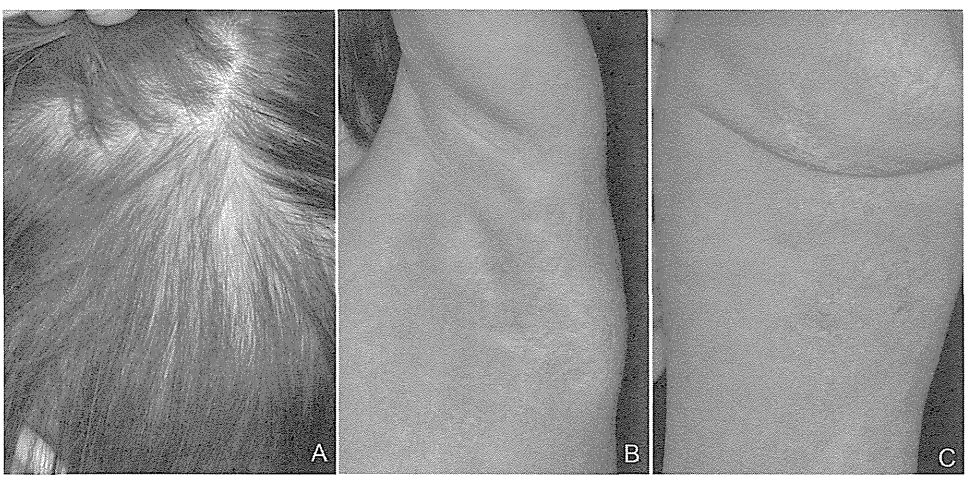

Fig. 1. Skin manifestation in the patient. (A) Hair loss on the left temporal scalp. (B, C) Small whitish depigmented spots, slightly depressed from the skin surface, distributed linearly on the left side of the armpit (B) buttocks and lower limbs (C).

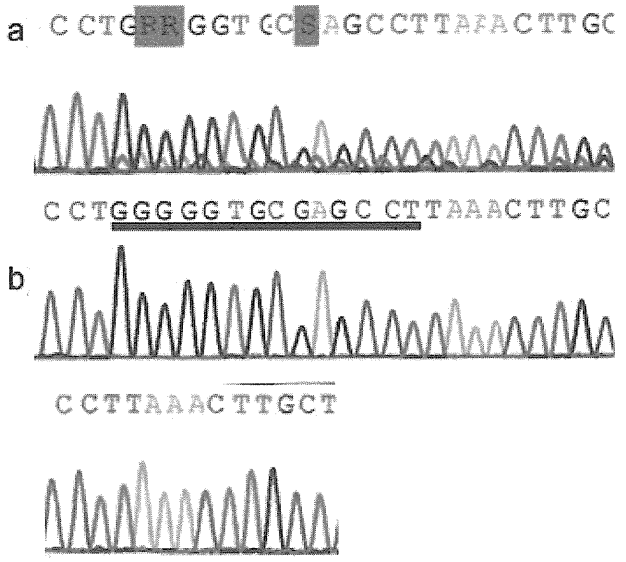

Fig. 2. Molecular basis of focal dermal hypoplasia (FDH). (a) Sequencing of exon 14 of the *PORCN* gene in the patient's DNA reveals c.1179_1193 del mutation. (b) Sequencing of control DNA shows the wild-type and mutant sequences.

and telangiectasias. It is presumed to be lethal in men who are fully hemizygous for a mutation in *PORCN* (4). FDH generally involves both sides of the body. Only 6 cases of unilateral FDH have been published (8–10). Recently, Maalouf et al. (8) reviewed all cases of unilateral FDH and found no side predeliction. One case was male (17%) and the other 5 were females (83%). Moreover, they described that gene sequence analysis on the *PORCN* gene detected a novel heterogeneous mutation in exon 10, c.854-855insACCTGAC [p.T285fsX316]. In addition, a substantial majority of cases of FDH have previously been reported to result from post-zygotic mutations (11). In the present case, sequencing analysis of the entire coding sequences of *PORCN* gene revealed a novel deletion mutation at exon 14 (c.1179_1193 del). As a ratio of 5/26 mutant vs. wild-type alleles was found, a post-zygotic mutation is the likely cause of the syndrome in our case. A germline mutation would have resulted in a 1:1 distribution of both alleles in functional X-chromosome-mosaicism as described previously by Bornholdt et al. (11). Although we did not perform the X-chromosome inactivation analysis using DNA extracted from the affected and non-affected skin, the present case suggests that the deletion mutation at exon 14 might be connected with the unilateral involvement of FDH. To confirm our hypothesis, further case reports and molecular studies of patients with unilateral FDH are necessary.

REFERENCES

1. Clements SE, Wessagowit V, Lai-Cheong JE, Arita K, McGrath JA. Focal dermal hypoplasia resulting from a new nonsense mutation, p.E300, in the PORCN gene. J Dermatol Sci 2008; 49: 39–42.
2. Lasocki AL, Stark Z, Orchard D. A case of mosaic Goltz syndrome (focal dermal hypoplasia) in a male patient. Australas J Dermatol 2011; 52: 48–51.
3. Buchner SA, Itin P. Focal dermal hypoplasia syndrome in a male patient: report of a case and histologic and immunohistochemical studies. Arch Dermatol 1998; 128: 1078–1082.
4. Yoshihashi H, Ohki H, Torii C, Ishiko A, Kosaki K. Survival of a male mosaic for PORCN mutation with mild focal dermal hypoplasia phenotype. Pediatr Dermatol 2011; 28: 550–554.
5. Grzeschik KH, Bornholdt D, Oeffner F, König A, del Carmen Boente M, Enders H, et al. Deficiency of PORCN, a regulator of Wnt signaling, is associated with focal dermal hypoplasia. Nat Genet 2007; 39: 833–835.
6. Carcicasole A, Ferraro T, Rimland JM, Terstappen GC. Molecular cloning and initial characterization of the MG61/PORC gene, the human homologue of the Drosophila segment polarity gene Porcupine. Gene 2002; 288: 147–157.
7. Hoffman K. A superfamily of membrane-bound O-acyltransferases with implications for wnt signaling. Trends Biochem Sci 2000; 25: 111–112.
8. Maalouf D, Mégarbané H, Chouery E, Nasr J, Badens C, Lacoste C, Grzeschik KH, Mégarbané A. A novel mutation in the PORCN gene underlying a case of almost unilateral focal dermal hypoplasia. Arch Dermatol 2012; 148: 85–88.
9. Aoyama M, Sawada H, Shintani Y, Isomura I, Morita A. Case of unilateral focal dermal hypoplasia (Goltz syndrome). J Dermatol 2008; 35: 33–35.
10. Tenkir A, Teshome S. Goltz syndrome (focal dermal hypoplasia) with unilateral ocular, cutaneous and skeletal features: case report. BMC Ophthalmol 2010; 10: 28.
11. Bornholdt D, Oeffner F, König A, Happle R, Alanay Y, Ascherman J, et al. PORCN mutations in focal dermal hypoplasia: coping with lethality. Hum Mutat 2009; 30: E618–628.

Int J Hematol (2013) 97:30–36
DOI 10.1007/s12185-012-1239-y

Ras/MAPK syndromes and childhood hemato-oncological diseases

Yoko Aoki · Yoichi Matsubara

Received: 3 October 2012 / Revised: 3 December 2012 / Accepted: 4 December 2012 / Published online: 19 December 2012

Abstract Noonan syndrome (NS) is an autosomal-dominant disease characterized by distinctive facial features, webbed neck, cardiac anomalies, short stature and cryptorchidism. NS exhibits phenotypic overlap with Costello syndrome and cardio-facio-cutaneous (CFC) syndrome. Germline mutations of genes encoding proteins in the RAS/mitogen-activated protein kinase (MAPK) pathway cause NS and related disorders. Germline mutations in *PTPN11*, *KRAS*, *SOS1*, *RAF1*, and *NRAS* have been identified in 60–80 % of NS patients. Germline mutations in *HRAS* have been identified in patients with Costello syndrome and mutations in *KRAS, BRAF,* and *MAP2K1/2* (MEK1/2) have been identified in patients with CFC syndrome. Recently, mutations in *SHOC2* and *CBL* have been identified in patients with Noonan-like syndrome. It has been suggested that these syndromes be comprehensively termed RAS/MAPK syndromes, or RASopathies. Molecular analysis is beneficial for the confirmation of clinical diagnoses and follow-up with patients using a tumor-screening protocol, as patients with NS and related disorders have an increased risk of developing tumors. In this review, we summarize the genetic mutations, clinical manifestations, associations with malignant tumors, and possible therapeutic approaches for these disorders.

Keywords RAS/MAPK signaling pathway · RASopathies · Oncogene · RAS · RAF · MEK

Y. Aoki (✉) · Y. Matsubara
Department of Medical Genetics,
Tohoku University School of Medicine,
1-1 Seiryo-machi, Sendai 980-8574, Japan
e-mail: aokiy@med.tohoku.ac.jp

Introduction

Noonan syndrome (NS, MIM 163950) was first described by Jacqueline Noonan, a pediatric cardiologist, in 1962. NS is an autosomal dominant disorder characterized by short stature, facial dysmorphism and congenital heart defects. The distinctive facial features that manifest in NS include a webbed or short neck, hypertelorism, downslanting palpebral fissures, ptosis and low-set, posteriorly rotated ears [1, 2]. Congenital heart defects, including pulmonary valve stenosis, occur in 50–80 % of individuals. Hypertrophic cardiomyopathy is observed in 20 % of affected individuals. Other clinical manifestations include cryptorchidism, bleeding tendency, mild intellectual disability, deafness, and hydrops fetalis. The incidence of this syndrome is estimated to be between 1 in 1,000 and 1 in 2,500 live births [3]. NS is known to be associated with juvenile myelomonocytic leukemia (JMML), a myeloproliferative disorder characterized by excessive production of myelomonocytic cells [1].

The phenotypic features of NS are similar to those of Costello and cardio-facio-cutaneous (CFC) syndromes. Costello syndrome (MIM 218040) was originally described by Costello in 1971 [4] and explored further by the same author in 1977 [5]. Patients with Costello syndrome have distinctive facial characteristics, including full lips, a large mouth, and a full nasal tip, and exhibit mental retardation, high birth weight, neonatal feeding problems, curly hair, nasal papillomata, and soft skin with deep palmar and plantar creases [6]. Cardiac defects include hypertrophic cardiomyopathy, congenital heart defects and arrhythmia. Children and young adults with Costello syndrome have an increased risk of malignancy, which can be as high as approximately 17 % [7].

CFC syndrome (MIM 115150) was first described in 1986 [8], and the question of whether CFC and NS are

distinct disorders or different phenotypes of the same condition is controversial. CFC syndrome is characterized by distinctive facial features, mental retardation, heart defects (pulmonic stenosis, atrial septal defect, and hypertrophic cardiomyopathy) and ectodermal abnormalities, such as sparse, friable hair, hyperkeratotic skin lesions and a generalized ichthyosis-like condition [9]. Typical facial characteristics include a high forehead with bitemporal constriction, hypoplastic supraorbital ridges, downslanting palpebral fissures, a depressed nasal bridge and posteriorly angulated ears with prominent helices.

NS with multiple lentigines was formerly referred to as LEOPARD syndrome. LEOPARD is an acronym for the cardinal features of the syndrome, which include multiple Lentigines, Electrocardiographic conduction abnormalities, Ocular hypertelorism, Pulmonary stenosis, Abnormal genitalia, Retardation of growth and sensorineural Deafness [10].

RAS GTPases are essential mediators in signaling pathways that convey extracellular stimuli from cell surface receptors to the cell. The Ras subfamily consists of classical Harvey-RAS (HRAS), Kirsten-RAS (KRAS) and neuroblastoma RAS (NRAS). Other distinct members include R-RAS, TC21 (R-RAS2), M-RAS (R-RAS3), Rap1A, Rap1B, Rap2A, Rap2B, RalA and RalB [11]. The RAS/mitogen-activated protein kinase (MAPK) pathway is an essential signaling pathway that controls cell proliferation, differentiation and survival. Recent studies have revealed that dysregulation of the RAS/MAPK pathway causes clinically overlapping genetic disorders, including NS, Costello syndrome, CFC syndrome, NS with multiple lentigines, neurofibromatosis type I, and Legius syndrome [6, 12]. This review outlines the molecular aspects, clinical manifestations, association with malignant tumors, and possible treatments of NS, Costello syndrome and CFC syndrome.

Genes and mutations that underlie genetic syndromes involving dysregulation of the RAS/MAPK signaling pathway (Table 1)

Background

In 1994, linkage analysis of a large family with NS definitively established the first NS locus, which was defined as chromosomal bands 12q22-qter [13, 14]. In 2001, Tartaglia et al. [15] identified missense mutations in *PTPN11*, which encodes the tyrosine phosphatase SHP-2, in individuals with NS. Gain-of-function mutations in *PTPN11* have been identified in approximately 50 % of individuals with clinically diagnosed NS [16–18] (Fig. 1). In contrast, loss-of-function or dominant negative mutations in *PTPN11* have been reported in patients with NS with multiple lentigines [10]. In 2005, we performed candidate gene analysis of proteins in the RAS/MAPK cascade and discovered germline mutations in *HRAS* in patients with Costello syndrome [19]. Subsequently, mutations in *KRAS*, *BRAF*, and *MAP2K1/2* have been identified in patients with CFC syndrome [20, 21], and mutations in *KRAS, SOS1, RAF1*, and *NRAS* have been identified in patients with NS [22–27] (Fig. 1). Recently, mutations in *SHOC2* [28] and *CBL* [29–31] have been identified in NS-like syndromes. These findings indicate that RAS and molecules downstream of RAS play essential roles in human development. It has been suggested that these syndromes be comprehensively termed 'RAS/MAPK syndromes' or 'RASopathies' [6, 12].

Table 1 Summary of RAS/MAPK syndromes

Disorder	MIM	Inheritance	Gene(s) mutated
NS	163950	AD	PTPN11, KRAS, SOS1, RAF1, NRAS
Noonan-like disorder with loose anagen hair	607721	AD	SHOC2
NS-like disorder	613563	AD	CBL
Costello syndrome	218040	AD	HRAS
Cardio-facio-cutaneous (CFC) syndrome	115150	AD	BRAF, MEK1, MEK2, KRAS
Neurofibromatosis type I	162200	AD	NF1
NF-1 like syndrome (Legius syndrome)	611431	AD	SPRED1
NS with multiple lentigines (LEOPARD syndrome)	151100	AD	PTPN11, RAF1, BRAF
Hereditary gingival fibromatosis	135300	AD	SOS1
Capillary malformation-arteriovenous malformation	608354	AD	RASA1

MIM Mendelian inheritance in man, *AD* autosomal dominant, *LEOPARD* multiple Lentigines, Electrocardiographic conduction abnormalities, Ocular hypertelorism, Pulmonary stenosis, Abnormal genitalia, Retardation of growth and sensorineural Deafness

Genes and mutations

PTPN11

SHP-2, the product of *PTPN11*, is a widely expressed cytoplasmic tyrosine phosphatase that has been implicated in signal transduction pathways elicited by growth factors, cytokines, hormones and the extracellular matrix [32]. SHP-2 comprises a tandem array of two SH2 domains at its N-terminus, a catalytic domain in the middle, and a C-terminal domain that contains tyrosine phosphorylation

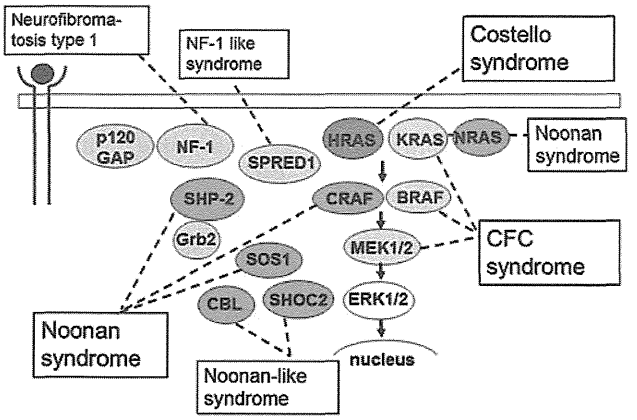

Fig. 1 RAS/MAPK cascade and disorders involving germline mutations of related genes

sites. Most mutations identified in NS were clustered in exons 3, 4, 7, 8, 12 and 13. Y63C, Q79R, N308D, and N308S were the most common mutations [6, 33]. T73I has been frequently identified in NS patients with JMML. Specific mutations (Y279C, A461T, G464A, T468M, D498W and Q510P) have been identified in NS with multiple lentigines.

Mutations that have been previously identified in NS are located in the interacting face of the N-SH2 domain and phosphatase domain, suggesting that they are gain-of-function mutations that enhance phosphatase activity. SHP-2 mutants associated with leukemia were more catalytically active than mutants identified in NS patients, suggesting that a high level of SHP-2 activation is associated with neoplastic diseases, whereas a lower level of SHP-2 activation causes NS [17, 34–36]. Mutations identified in NS with multiple lentigines have been shown to be catalytically inactive or dominant negative [36–38].

SOS1

SOS1 is a ubiquitously expressed guanine nucleotide exchange factor (GEF) that is responsible for the activation of RAS proteins by catalyzing GDP/GTP exchange. Mutations in *SOS1* have been identified in 8–14 % of patients with NS [25, 27], and the biochemical characterization of SOS1 mutants has indicated enhanced protein function and increased downstream signaling. Compared with other NS patients, the incidence of short stature and intellectual disability is lower in patients who tested positive for an *SOS1* mutation [39].

RAF1

RAF1 is a member of the RAS serine–threonine kinase family. Mutations in *RAF1* have been identified in 3–17 % of patients with NS and a small number of patients with NS with multiple lentigines [23, 24]. Mutations identified in NS were clustered in conserved region (CR) 2, which contains an inhibitory phosphorylation site (serine at position 259; S259). RAF1 mutations located in the CR2 domain caused a decrease in the phosphorylation of S259, leading to partial ERK activation [39]. Notably, 70 % of patients with *RAF1* mutations exhibit hypertrophic cardiomyopathy [23, 24, 39, 40].

HRAS

Individuals with *HRAS* mutations are diagnosed as having Costello syndrome, and heterozygous *HRAS* mutations have been identified in more than 90 % of patients with this syndrome [6, 19]. Germline mutations are clustered in codons 12 and 13, and the G12S mutation is the most frequent (80 %). *HRAS* germline mutations occur de novo. Somatic mosaicism for the G12S mutation has been reported in three individuals with clinical findings suggestive for Costello syndrome [41].

KRAS

Individuals with *KRAS* mutations exhibit variable phenotypes and are diagnosed with NS or CFC syndrome [20, 26, 42]. Mutations in codons 12, 13, and 61, which are frequent in somatic cancers, have rarely been identified as germline mutations, which is in contrast with *HRAS* germline mutations. V14I is a frequent mutation in NS, and D153V mutation has been identified in patients with NS or CFC syndrome [6]. The effects of *KRAS* germline mutations on the downstream pathway are less pronounced than the effects of somatic mutations [20, 26]

BRAF and MAP2K1/2 (MEK1/2)

Mutations in *BRAF* and *MAP2K1/2* have been identified in patients with CFC syndrome [20, 21]. *BRAF* mutations have also been identified in patients with a phenotype of NS with multiple lentigines. Somatic mutations in *BRAF* have been identified in 7 % of all cancers, including human malignant melanoma and colorectal cancer [43]. V600E mutation in the activation segment in the kinase domain (CR3) has been frequently identified in somatic cancers (>90 %). Germline mutations were clustered in the cysteine-rich domain (CR1 domain) and kinase domain. The distribution of the mutations identified in CFC syndrome partially overlapped with that of the mutations identified in cancers. Q257R and E501G are frequent mutations in CFC syndrome [6]. Germline mutations in *MAP2K1/2* are clustered in exons 2 and 3. ERK phosphorylation was

enhanced in cells transfected with mutant MEK1 or MEK2 [21]. Affected individuals harboring *BRAF* and *MAP2K1/2* mutations have the disorder as a result of a de novo mutation. One family transmitting an autosomal dominant germline mutation in *MAP2K2* has been reported [44].

SHOC2

SHOC2 is homologous to *soc2*, a gene discovered in *Caenorhabditis elegans*. The *soc2* gene encodes leucine-rich repeats [45] and acts as a positive modulator of the RAS/MAPK pathway [46]. In 2009, a gain-of-function missense mutation in *SHOC2*, c.4A > G (p.S2G), was identified in patients with Noonan-like syndrome with loose anagen hair [28]. The clinical features associated with the S2G mutation are distinct from those associated with NS and include a high frequency of loose anagen hair, more severe intellectual disabilities, skin abnormalities, and a hypernasal voice [28, 47]. Wild-type SHOC2 is localized in the nucleus and cytoplasm, while the mutant protein (S2G) promoted aberrant N-myristoylation, localized to the plasma membrane and resulted in ERK activation [28].

NRAS

A germline mutation in *NRAS* has been reported in a patient with autoimmune lymphoproliferative syndrome. Germline mutations in *NRAS* have been reported in four of 917 NS patients (0.4 %) who were negative for previously known mutations [22]. The amino acid changes identified in NS patients were I24N, P34L, T50I and G60E [22, 48, 49]. Cells carrying T50I and G60E mutations and oncogenic G12V displayed enhanced MEK and ERK phosphorylation when serum was added to the growth medium [22].

CBL

Casitas B-cell lymphoma (CBL) is the cellular homolog of the v-Cbl transforming gene of the Cas NS-1 murine leukemia virus. CBL functions primarily as an E3 ubiquitin ligase and is responsible for the intracellular transport and degradation of a large number of proteins. The majority of *CBL* somatic mutations have been reported in myelodysplastic syndromes/myeloproliferative disorders, including chronic myelomonocytic, juvenile myelomonocytic and atypical chronic myeloid leukemias. Germline mutations in *CBL* have been identified in JMML patients who displayed a variable combination of dysmorphic features reminiscent of the facial gestalt of NS [29–31].

Association of tumors and hematologic malignancies in patients with germline mutations in genes within the RAS/MAPK pathway (Table 2)

Somatic mutations in genes in the RAS pathway, including *PTPN11*, *HRAS*, *KRAS*, *NRAS*, *BRAF* and *CBL*, have been identified in a variety of solid tumors and hematologic malignancies. NS and related disorders are known to cause a predisposition to cancer. The precise frequency of tumor predisposition in mutation-positive patients remains unknown.

It has been reported that the *PTPN11* mutations in patients with NS are frequently associated with hematologic malignancies, including acute lymphoblastic leukemia and JMML. The frequency of association with tumors remains unknown. In a summary of the literature, Kratz et al. [50] reported that 45 of 1,151 patients (3.9 %) with NS (mutation status unknown) developed cancer; of these, eight patients presented with neuroblastoma, and eight presented with acute lymphoblastic leukemia. The other cancers identified included six gliomas, six rhabdomyosarcoma, three acute myeloid leukemias, three testicular cancers, two non-Hodgkin lymphomas and two colon cancers. *PTPN11* mutations in patients with NS have been shown to be associated with myeloproliferative disorder, and with a benign course in 40 % of such patients, and an aggressive course in 15 % [50]. It remains unknown why gain-of-function mutations in *PTPN11* enhance the proliferation of specific lineages in hematologic malignancies.

Approximately, 10–15 % of patients with Costello syndrome develop malignant tumors, including rhabdomyosarcoma, neuroblastoma (in infants) and transitional cell carcinoma of the bladder (in adolescents and young adults) [6]. A tumor screening protocol for patients with Costello syndrome has been proposed [7]. Notably, *HRAS* mutations were originally identified in bladder carcinoma cell lines. It remains unknown why patients with *HRAS* germline mutations develop bladder carcinomas.

Little attention had been given to the development of tumors in patients with CFC syndrome until molecular analysis became available. Two CFC patients with *BRAF* mutations were reported to have developed acute lymphoblastic leukemia [20, 51], and one CFC patient with a *BRAF* mutation was reported to have developed non-Hodgkin lymphoma [52]. Somatic *BRAF* mutations in hematologic malignancies do not occur frequently, but they are substantially reported. Recently, *BRAF* mutations have been identified in Langerhans cell histiocytosis [53]. It is possible that the role of BRAF in hematologic malignancies may indicate that BRAF plays roles in other malignancies beyond solid tumors. As for *MAP2K1/2*, one patient with a *MAP2K1* mutation developed hepatoblastoma [54].

Table 2 Disorders involving germline and somatic mutations in genes of the RAS/MAPK cascade

Gene	Germline mutations		Somatic mutations
	Disorders	Associated tumors	Tumors and related disorders
PTPN11	NS, NS with multiple lentigines (LEOPARD syndrome)	JMML, myeloproliferative disorders [50]	JMML, AML, ALL, MDS, CML, solid tumors
SOS1	NS	Rhabdomyosarcoma (1 pt), Sertoli cell tumor (1 pt), granular cell tumors (1 pt) [55]	Rare (astrocytoma, lung cancer)
RAF1	NS, NS with multiple lentigines (LEOPARD syndrome)	–	Rare (AML, lung cancer, ovarian cancer, colon cancer)
SHOC2	Noonan-like disorder with loose anagen hair	–	–
NRAS	NS	–	Hematologic malignancies
CBL	NS-like disorder	JMML [30, 31]	JMML, CML, AML, MDS, lung cancer
HRAS	Costello syndrome	Rhabdomyosarcoma, neuroblastoma, bladder carcinoma, papillomata	Bladder carcinoma
KRAS	CFC syndrome, NS	JMML (1 pt) [26]	Pancreatic tumor, colon cancer, lung cancer, RAS-associated ALPS-like disease [63]
BRAF	CFC syndrome NS	ALL (2 pts) [20, 51], non-Hodgkin lymphoma (1 pt) [52]	Malignant melanoma, colon cancer, thyroid cancer, Langerhans cell histiocytosis [53]
MEK1	CFC syndrome	Hepatoblastoma (1 pt) [54]	–
MEK2	CFC syndrome	–	–

JMML juvenile myelomonocytic leukemia, *ALL* acute lymphoblastic leukemia, *AML* acute myelogenous leukemia, *CML* chronic myelogenous leukemia, *MDS* myelodysplastic syndromes, *ALPS* autoimmune lymphoproliferative syndrome

Germline mutations in *CBL* have been identified in JMML patients who displayed a variable combination of dysmorphic features reminiscent of the facial gestalt of NS. Facial appearances, psychomotor development, head circumference and skin abnormalities should be carefully observed in children with hematologic malignancies. A patient with a *KRAS* mutation who developed JMML has been reported [26]. It has been reported that three patients with *SOS1* germline mutations developed rhabdomyosarcoma (one patient), Sertoli cell tumors (one patient), and granular cell tumors (one patient) [55]. As far as we know, tumor association has not been reported in individuals with germline mutations in *SHOC2*, *NRAS*, and *RAF1*.

The natural history and predisposition for hematologic malignancies and solid tumors in adults with RAS/MAPK syndromes have not been clarified. We conducted a nationwide epidemiologic study on patients with Costello and CFC syndromes in 2009 [56]. The results showed that the total number of patients with Costello and CFC syndrome in Japan was estimated to be 99 (95 % confidence interval, 77–120) and 157 (95 % confidence interval, 86–229), respectively. An evaluation of 15 adult patients (18–32 years of age) revealed that one had recurrent bladder papillomata and another had multiple gallbladder polyps and a renal angioma. None of the examined patients developed malignant tumors. Twelve of 15 adult patients had moderate to severe mental retardation, but eleven live at home, and 10 can walk independently, suggesting that a portion of adult patients may be unrecognized and the number of adult patients is likely underestimated. Therefore, the prognosis, including the frequency of malignant tumors, remains to be elucidated in adults with germline mutations in *RAS* and *RAF*.

Conclusions

The identification of the causative genes underlying NS and related disorders has facilitated the molecular diagnosis of these disorders, allowed the evaluation of the genotype–phenotype relationship and helped develop possible therapeutic approaches. In approximately 10–30 % of patients with RAS/MAPK syndromes, no mutations were identified. The introduction of exome sequencing will lead to the identification of novel genes involved in these disorders.

The regulation and inhibition of the RAS/MAPK pathway have been well studied in cancer research. Inhibitors of the RAS/MAPK cascade may provide opportunities to therapeutically treat disorders involving dysregulation of the RAS/MAPK pathway [57]. Indeed, MEK inhibitors ameliorated the phenotype of mice models for NS (mutations in *SOS1* and *RAF1*) [58, 59] and Costello syndrome (mutation in *HRAS*) [60]. An inhibitor of mTOR has been shown to reverse heart defects in a mouse model for NS with multiple lentigines [61]. HMG-CoA reductase inhibitors have been used in clinical trials to treat cognitive